

## FATIGUE OF END FLOOR BEAM CONNECTION PLATE OF STIFFENED ARCH BRIDGE

By Ichiro OKURA\*, Toshihisa SHIBAIKE\*\* and Yukio MAEDA\*\*\*

In a stiffened arch bridge, a fatigue crack was detected at a plate connecting the top flange of an end floor beam to the main girder. In this paper, the stress which induced the fatigue crack is evaluated by the three-dimensional framed-structural analysis of the stiffened arch bridge, and then the relation between the stress and its overall behavior is discussed.

*Keyword* : stiffened arch bridge, fatigue, end floor beam connection plate, three-dimensional framed-structural analysis

### 1. INTRODUCTION

In a stiffened arch bridge, a fatigue crack was detected at the welding part of a plate connecting the top flange of an end floor beam to the main girder, as shown in Fig. 1. It was initiated at the connection plate at each end of the end floor beams. Repeated relative difference in displacement in the bridge-axis direction between the main girder and the floor system is considered to be one of the factors to initiate such a fatigue crack<sup>1)</sup>. But, the mechanism of the development of the relative difference in displacement is not clear. Furthermore, the other factors may have influenced the initiation of the fatigue crack. In this paper, the stress which induced the fatigue crack at the connection plate is evaluated by the three-dimensional framed-structural analysis of the stiffened arch bridge, and then the relation between the stress and its overall behavior is discussed.

### 2. THREE-DIMENSIONAL FRAME ANALYSIS OF STIFFENED ARCH BRIDGE

#### (1) Three-dimensional framed structure

A general picture of the stiffened arch bridge in which the fatigue cracks were actually detected is shown in Fig. 2. The

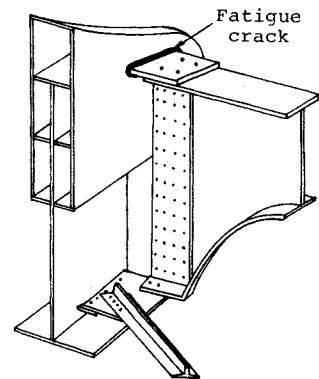


Fig.1 Fatigue Crack at Connection Plate.

\* Member of JSCE, Dr. Eng., Research Associate, Department of Civil Engineering, Osaka University (Yamada-Oka 2-1, Suita, Osaka 565)

\*\* Member of JSCE, M. Eng., Civil Engineering Bureau, Osaka Prefectural Government (Otemae, Higashi-ku, Osaka 540)

\*\*\* Member of JSCE, Dr. Eng., Professor, Department of Civil Engineering, Kinki University (Kowakae 3-4-1, Higashiosaka, Osaka 577)

bridge was designed as the second class bridge in the Japanese Specification for Highway Bridges<sup>2)</sup>. The span length, arch rise, main girder spacing and floor beam spacing are 79.2 m, 12.4 m, 8.05 m and 6.6 m, respectively. The roadway is 7.0 m wide and has a single lane on each side. The sidewalks are not provided. The main girders, floor beams, stringers and upper lateral struts have all an I-section, and the arch ribs, hangers and lower lateral bracings have a box-section, H-section and T-section, respectively. The steel of the main girders, floor beams and arch ribs is JIS SM 50 A, and the steel of the other members is JIS SS 41.

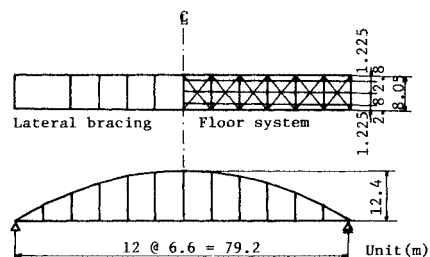


Fig. 2 General Picture of Stiffened Arch Bridge.

The stiffened arch bridge is modelled into a three-dimensional framed structure, based on the following assumptions.

- i) Connections between the hanger and the arch rib, or between the hanger and the main girder are generally assumed to be hinged joints in the design of stiffened arch bridges. But, the connections of the present stiffened arch bridge may be regarded as rigid joints, because gusset plates and high strength bolts are used for the connections.
- ii) The centroids of the members do not always coincide at each joint. In this analysis, the eccentricities among the members are neglected except the one between the main girder and the arch rib at the end support. An offset beam element<sup>3)</sup> is used to take into account the eccentricity between the main girder and the arch rib at the end support.

Lower lateral bracings are generally designed as secondary members to resist lateral loads such as wind or earthquake. In stiffened arch bridges, they have such an effect that reduces the relative difference in displacement in the bridge-axis direction between the main girders and the floor system, because they can carry a part of the axial force of the main girders. Then, to examine the effect of the lower lateral bracings, calculations are done for a model taking into account the lower lateral bracings and then for the one not taking into account them. The latter and former are called structural models (I) and (II), respectively.

## (2) Applied loads

Loads for the fatigue design are not specified in the Japanese Specification for Highway Bridges<sup>2)</sup>. Information on traffic loads of the present stiffened arch bridge was not available. Then, the calculations are carried out for the following three kinds of loads.

(A) : Dead loads such as reinforced concrete slab, asphalt pavement, curbs and hand rails are applied.  
 (B) and (C) : A T-load for the design of slab and floor system specified in the Japanese Specification for Highway Bridges moves on the bridge along the stringers as a concentrated load. The case where one T-load moves along the stringer nearest the connection plate at one end of an end floor beam, and the case where it moves along the farthest stringer are called applied loads (B) and (C), respectively. Since the stiffened arch bridge is the second class bridge, the magnitude of the T-load is 137.3 kN.

## (3) Stresses at connection plate

Stresses produced at the connection plate of an end floor beam are calculated from the internal stress resultants of the end floor beam. Their values are listed in Table 1. Referring to Fig. 3, the stress components of  $\sigma_x$ ,  $\sigma_y$ ,  $\sigma_z$ ,  $\tau_y$  and  $\tau_z$  in Table 1 correspond to  $N_x$ ,  $M_y$ ,  $M_z$ ,  $Q_y$  and  $M_x$ , respectively. The shearing stress component corresponding to  $Q_z$  is neglected, because the end floor beam is an I-section. The values for applied loads (B) and (C) in Table 1 are the differences between the maximum and minimum stresses when one T-load passes through the bridge.

It can be seen from Table 1 that in each combination of applied loads and structural models, the stress component  $\sigma_z$  is higher than any other stress component. Accordingly, the in-plane bending stress  $\sigma_z$

Table 1 Stress Components at Connection Plate.

Applied load	Structural model	Stress components (MPa)					
		$\sigma_x$	$\sigma_y$	$\sigma_z$	$\tau_{xy}$	$\tau_{yz}$	$\tau_{xz}$
A	I	0.1	0.7	254.5	2.0	0.2	
	II	0.1	0.7	248.9	2.0	0.2	
B	I	0.0	2.2	36.3	0.3	0.2	
	II	0.0	2.1	34.4	0.2	0.2	
C	I	0.0	2.1	31.6	0.2	0.1	
	II	0.0	2.0	29.4	0.2	0.1	

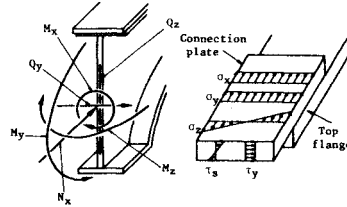


Fig.3 Internal Stress Resultants and Stress Components.

produced at the connection plate is considered to be the stress governing the initiation of the fatigue crack. On the other hand, since the variation of  $\sigma_z$  is small between structural models ( I ) and ( II ), the lower lateral bracings do not influence a decrease in  $\sigma_z$  so much.

( 4 ) Mechanism of initiation of in-plane bending stress  $\sigma_z$

The variation of  $\sigma_z$  in a passage of one T-load on the bridge is shown in Fig. 4 for both of applied loads (B) and (C). Even when the load is on the end floor beam,  $\sigma_z$  occurs. This can be explained as follows. When the load is on the end floor beam, a rotation about the bridge-axis is produced at the connection between the end floor beam and the main girder. Since the arch rib is connected askew to the main girder, this rotation produces a rotation about the vertical axis, which induces an out-of-plane bending moment at the connection of the end floor beam, resulting in the initiation of  $\sigma_z$ . After the load has passed through the end floor beam, this phenomenon disappears, because the load which is transferred to the end floor beam decreases rapidly.

On the other hand, the mechanism of the initiation of  $\sigma_z$  when the load is on the stringer can be explained as follows. Referring to the drawing inserted in Fig. 4, the relative difference in displacement in the bridge-axis direction between the main girder and the adjacent stringer, and the displacement in the direction perpendicular to the bridge-axis of the intersection of the hanger nearest the end support and the arch rib are denoted by  $\Delta u$  and  $w$ , respectively. The variation of  $\Delta u$  and  $w$  are shown in Figs. 5 and 6, respectively. It can be expected from Figs. 4, 5 and 6 that there will exist the following relation among  $\sigma_z$ ,  $\Delta u$  and  $w$  when one T-load is moving on the bridge :

$$\sigma_z = k_1 \Delta u + k_2 w + c \dots\dots\dots ( 1 )$$

where  $k_1$ ,  $k_2$  and  $c$  = coefficients.

The regression analysis gives the values of  $k_1$ ,  $k_2$  and  $c$  as shown in Table 2. The values of  $\sigma_z$ ,  $\Delta u$  and  $w$ , when the T-load is on the end floor beam, are not used in the regression analysis. The values of  $\sigma_z$ , which are obtained by substitution of the values of  $\Delta u$  and  $w$  shown in Figs. 5 and 6 into Eq. ( 1 ), are also shown in broken lines in Fig. 4. The values of  $\sigma_z$  obtained from Eq. ( 1 ) approximate very well to the ones which are directly obtained by the three-dimensional frame analysis. Accordingly, when one T-load is moving on the stringer,  $\sigma_z$  is induced by the following two factors :

- i) the relative difference in displacement in the bridge-axis direction between the main girder and the stringer, and
- ii) the displacement of the arch rib in the direction perpendicular to the bridge-axis.

The mechanism of the initiation of the relative difference in displacement in the bridge-axis direction between the main girder and the stringer can be explained as follows. In stiffened arch bridges, since the main girders are always subjected to tensile axial forces, they are stretched in the bridge-axis direction. Accordingly, a relative difference in displacement in the bridge-axis direction between the main girder and the stringer is produced. On the other hand, the displacement of the arch rib in the direction perpendicular to the bridge-axis is produced by the overall torsional deformation of the stiffened arch frame.

As has been mentioned above, the in-plane bending stress  $\sigma_z$  induced at the connection plate is caused by the local behavior of the connection of the end floor beam and arch rib, when the load is on the end floor beam, and by the three-dimensional overall behavior of the stiffened arch bridge, when the load is on the

Table 2 Values of Coefficients.

	$k_1$ (MPa/cm)	$k_2$ (MPa/cm)	$c$ (MPa)
(B, I)	405.4	39.9	1.4
(B, II)	534.4	35.0	-0.0
(C, I)	847.4	40.9	-0.3
(C, II)	457.6	34.8	1.2

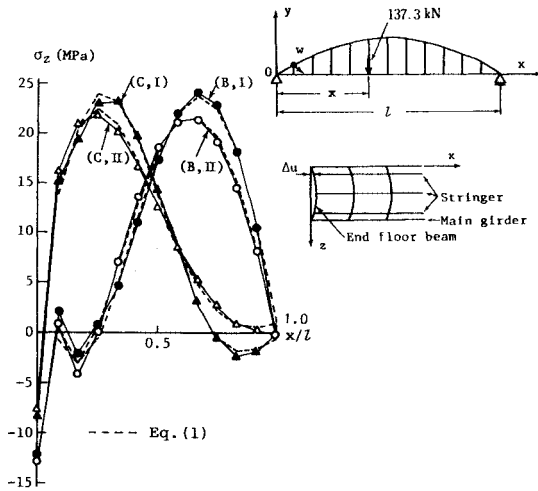


Fig. 4 Variation of  $\sigma_z$ .

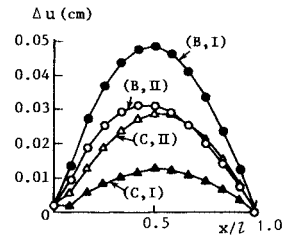


Fig. 5 Variation of  $\Delta u$ .

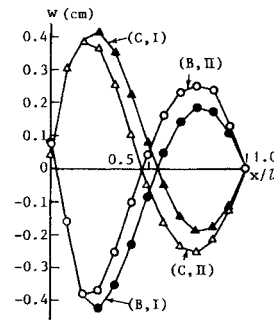


Fig. 6 Variation of  $w$ .

stringer.

### 3. CONCLUSION

The stress which induced the fatigue crack at the plate connecting the top flange of an end floor beam to the main girder in a stiffened arch bridge, is the in-plane bending stress produced on the plate. This stress is caused by the local behavior of the connection of the end floor beam or by the three-dimensional overall behavior of the stiffened arch bridge.

#### REFERENCES

- 1) Fisher, J.W. : Fatigue and Fracture in Steel Bridges, John Wiley & Sons Inc., pp.279~289, 1984.
- 2) Japan Road Association : Specification for Highway Bridges, 1980.
- 3) Kawai, T. et al. : Plate Structure Analysis, Baihukan Publisher, Tokyo, pp.48~52, 1973.

(Received May 9 1986)